Non-integrability vs. integrability in pentagram maps

Boris Khesin [a,*], Fedor Soloviev [b,c]

[a] *Department of Mathematics, University of Toronto, Toronto, ON M5S 2E4, Canada*
[b] *The Fields Institute, Toronto, ON, Canada*
[c] *CRM - Université de Montréal, Montreal, QC, Canada*

A B S T R A C T

We revisit recent results on integrable cases for higher-dimensional generalizations of the 2D pentagram map: short-diagonal, dented, deep-dented, and corrugated versions, and define a universal class of pentagram maps, which are proved to possess projective duality. We show that in many cases the pentagram map cannot be included into integrable flows as a time-one map, and discuss how the corresponding notion of discrete integrability can be extended to include jumps between invariant tori. We also present a numerical evidence that certain generalizations of the integrable 2D pentagram map are non-integrable and present a conjecture for a necessary condition of their discrete integrability.

© 2014 Elsevier B.V. All rights reserved.

The goal of this paper is three-fold. First we revisit the recent progress in finding integrable generalizations of the 2D pentagram map. Secondly, we discuss a natural framework for the notion of a discrete integrable Hamiltonian map. It turns out that the Arnold–Liouville theorem on existence of invariant tori admits a natural generalization to allow discrete dynamics with jumps between invariant tori, which is relevant for many pentagram maps. Lastly, we define a universal class of pentagram-type maps, describe a projective duality for them, and present a numerical evidence for non-integrability of several pentagram maps in 2D and 3D. In view of many new integrable generalizations found recently, a search for a non-integrable generalization of the pentagram map was brought into light, and the examples presented below might help focusing the efforts for such a search.
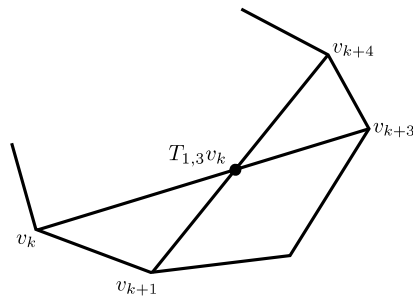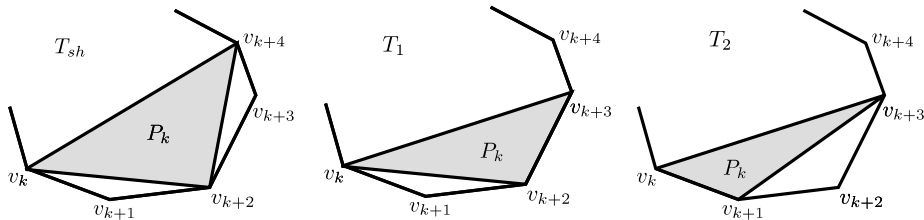
1. Types of pentagram maps

Recall that the pentagram map is a map on plane convex polygons considered up to their projective equivalence, where a new polygon is spanned by the shortest diagonals of the initial one, see [1]. It exhibits quasi-periodic behavior of (projective classes of) polygons in 2D under iterations, which indicates hidden integrability. The integrability of this map was proved in [2], see also [3].

While the pentagram map is in a sense unique in 2D, its generalizations to higher dimensions allow more freedom. It turns out that while there seems to be no natural generalization of this map to polyhedra, one can suggest several natural integrable extensions of the pentagram map to the space of generic twisted polygons in higher dimensions.

Definition 1.1. A *twisted n-gon* in a projective space $\mathbb{P}^d$ with a monodromy $M \in SL_{d+1}$ is a doubly-infinite sequence of points $v_k \in \mathbb{P}^d$, $k \in \mathbb{Z}$, such that $v_{k+n} = M \circ v_k$ for each $k \in \mathbb{Z}$, and where M acts naturally on $\mathbb{P}^d$. We assume that the vertices v_k

---

* Corresponding author.
  E-mail address: khesin@math.toronto.edu (B. Khesin).

Fig. 1. Deeper pentagram map $T_{1,3}$ in 2D.

Fig. 2. Different diagonal planes in 3D: for T_{sh}, T_1, and T_2.

are in general position (i.e., no $d + 1$ consecutive vertices lie in the same hyperplane in $\mathbb{P}^d$), and denote by $\mathscr{P}_n$ the space of generic twisted n-gons considered up to the projective equivalence.

We use projective spaces defined over reals $\mathbb{R}$ (as the easiest ones to visualize), over complex numbers $\mathbb{C}$ (to describe algebraic–geometric integrability), and over rational numbers $\mathbb{Q}$ (to perform a non-integrability test). All definitions below work for any base field. General pentagram maps are defined as follows.

Definition 1.2. We define 3 types of diagonal hyperplanes for a given twisted polygon (v_k) in $\mathbb{P}^d$. (a) The *short-diagonal hyperplane* P_k^{sh} is defined as the hyperplane passing through d vertices of the n-gon by taking every other vertex starting with v_k:

$$P_k^{\text{sh}} := (v_k, v_{k+2}, v_{k+4}, \ldots, v_{k+2(d-1)}).$$

(b) The *dented diagonal plane hyperplane* P_k^m for a fixed $m = 1, 2, \ldots, d-1$ is the hyperplane passing through all vertices from v_k to v_{k+d} but one, by skipping only the vertex v_{k+m}:

$$P_k^m := (v_k, v_{k+1}, \ldots, v_{k+m-1}, v_{k+m+1}, v_{k+m+2}, \ldots, v_{k+d}).$$

(c) The *deep-dented diagonal plane hyperplane* P_k^m for fixed positive integers m and $p \geq 2$ is the hyperplane as above that passes through consecutive vertices, except for one jump, when it skips $p - 1$ vertices $v_{k+m}, \ldots, v_{k+m+p-2}$:

$$P_k^{m,p} := (v_k, v_{k+1}, \ldots, v_{k+m-1}, v_{k+m+p-1}, v_{k+m+p}, \ldots, v_{k+d+p-2}).$$

(Here $P_k^{m,2}$ corresponds to P_k^m in (b).)
Now the corresponding *pentagram maps* T_{sh}, T_m, and $T_{m,p}$ are defined on generic twisted polygons (v_k) in $\mathbb{P}^d$ by intersecting d consecutive diagonal hyperplanes:

$$T v_k := P_k \cap P_{k+1} \cap \cdots \cap P_{k+d-1},$$

where each of the maps T_{sh}, T_m, and $T_{m,p}$ uses the definition of the corresponding hyperplanes P_k^{sh}, P_k^m, and $P_k^{m,p}$. These pentagram maps are generically defined on the classes of projective equivalence of twisted polygons $T : \mathscr{P}_n \to \mathscr{P}_n$.

Example 1.3. For $d = 2$ one can have only $m = 1$ and the definitions of T_{sh} and T_m coincide with the standard 2D pentagram map T_{st} in [1] (up to a shift in vertex numbering). The deep-dented maps $T_{1,p}$ in 2D are the maps $T_{1,p} v_k := (v_k, v_{k+p}) \cap (v_{k+1}, v_{k+p+1})$ obtained by intersecting deeper diagonals of twisted polygons, see Fig. 1.

For $d = 3$ the map T_{sh} uses the diagonal planes $P_k^{\text{sh}} := (v_k, v_{k+2}, v_{k+4})$, while for the dented maps T_1 and T_2 one has $P_k^1 = (v_k, v_{k+2}, v_{k+3})$ and $P_k^2 = (v_k, v_{k+1}, v_{k+3})$, respectively, see Fig. 2.

Theorem 1.4. *The short-diagonal T_{sh}, dented T_m and deep-dented $T_{m,p}$ maps are integrable in any dimension d on both twisted and closed n-gons in a sense that they admit Lax representations with a spectral parameter.*

The integrability of the standard 2D pentagram map $T_{\text{st}} := T_{\text{sh}} = T_m$ was proved in [2], while its Lax representation was found in [3]. In [4] integrability of the pentagram map for corrugated polygons (which we discuss below) was proved, which implies integrability of the maps $T_{1,p}$ in 2D.

For higher pentagram maps in any dimension d, their Lax representations with a spectral parameter were found in [5]. The dependence on spectral parameter was based on the scale invariance of such maps, which was proved in [5] for 3D, and in [6] for higher d. For the dented and deep-dented pentagram maps their Lax representations and scale invariance in any dimension d were established in [7]. We present formulas for those Lax representations in Section 2. Such representations with a spectral parameter provide first integrals of the maps (as the coefficients of the corresponding spectral curves) and allow one to use algebraic–geometric machinery to prove various integrability properties.

In [5,7] we proved that the proposed Lax representation implies algebraic–geometric integrability for the maps T_{sh}, T_1, T_2 in 3D. In particular, this means that the space of twisted n-gons in the complex space $\mathbb{CP}^3$ is generically fibered into (Zariski open subsets of) tori whose dimension is described in terms of n. In Section 3 we discuss features of the pentagram maps which emphasize their discrete nature.

Definition 1.5. More generally, one can define *generalized pentagram maps $T_{I,J}$* on (projective equivalence classes of) twisted polygons in $\mathbb{P}^d$, associated with $(d-1)$-tuples of integers I and J: the *jump tuple* $I = (i_1, \ldots, i_{d-1})$ determines which vertices define the diagonal hyperplanes P_k^I:

$$P_k^I := (v_k, v_{k+i_1}, \ldots, v_{k+i_1+\cdots+i_{d-1}}), \tag{1.1}$$

while the *intersection tuple* $J = (j_1, \ldots, j_{d-1})$ determines which hyperplanes to intersect in order to get the image of the point v_k:

$$T_{I,J}v_k := P_k^I \cap P_{k+j_1}^I \cap \cdots \cap P_{k+j_1+\cdots+j_{d-1}}^I.$$

In general, the integrability of $T_{I,J}$ is yet unknown, but there exists the following duality between such pentagram maps:

$$T_{I,J}^{-1} = T_{J^*,I^*} \circ Sh, \tag{1.2}$$

where I^* and J^* stand for the $(d-1)$-tuples taken in the opposite order and Sh is any shift in the indices of polygon vertices, see [7]. In particular, the maps $T_{I,J}$ and T_{J^*,I^*} are integrable or non-integrable simultaneously.

The pentagram maps T_{sh}, T_m, and $T_{m,p}$ considered above correspond to $J = (1, \ldots, 1)$ (cf. Definitions 1.2 and 1.5). The duality (1.2) of $T_{I,J}$ and T_{J^*,I^*} along with Theorem 1.4 implies integrability of the maps with $I = (1, \ldots, 1)$ and appropriate J's.

The simplest pentagram map which is neither short-diagonal, nor dented or deep-dented appears in dimension $d = 3$ and corresponds to $I = (2, 3)$ and $J = (1, 1)$. We conjecture that it is indeed non-integrable and outline supporting evidence from computer experiments in Sections 5 and 6, along with several other cases both integrable and not.

Remark 1.6. In [5,7] it was also proved that the continuous limit of any short-diagonal or dented pentagram map (and more generally, of any generalized pentagram map) in $\mathbb{RP}^d$ is the $(2, d + 1)$-KdV flow of the Adler–Gelfand–Dickey hierarchy on the circle. For 2D this is the classical Boussinesq equation on the circle: $u_{tt} + 2(u^2)_{xx} + u_{xxxx} = 0$, which appears as the continuous limit of the 2D pentagram map [2].

Remark 1.7. Note also that a different integrable generalization to higher dimensions was proposed in [4], where the pentagram map was defined not on generic, but on the so-called *corrugated* polygons. These are twisted polygons in $\mathbb{P}^d$, whose vertices v_{k-1}, v_k, v_{k+d-1}, and v_{k+d} span a projective two-dimensional plane for every $k \in \mathbb{Z}$. The pentagram map $T_{cor}v_k := (v_{k-1}, v_{k+d-1}) \cap (v_k, v_{k+d})$ on corrugated polygons turns out to be integrable and admits an explicit description of the Poisson structure, a cluster algebra structure, and other interesting features [4]. Furthermore, it turns out that the pentagram map T_{cor} can be viewed as a particular case of the dented pentagram map:

Theorem 1.8 ([7]). *This pentagram map T_{cor} is a restriction of the dented pentagram map T_m for any $m = 1, \ldots, d - 1$ from generic n-gons $\mathcal{P}_n$ in $\mathbb{P}^d$ to corrugated ones (or differs from it by a shift in vertex indices). In particular, these restrictions for different m coincide modulo an index shift.*

2. Formulas for Lax representations

In this section we recall explicit formulas of the Lax representation for pentagram maps. First we introduce coordinates on the space $\mathcal{P}_n$ of generic twisted n-gons in $\mathbb{P}^d$ considered over $\mathbb{C}$. For simplicity, we focus only on the case when $\gcd(n, d + 1) = 1$ (see the general case in [5,7]).

One can show that there exists a lift of the vertices $v_k = \phi(k) \in \mathbb{CP}^d$ to the vectors $V_k \in \mathbb{C}^{d+1}$ satisfying $\det(V_j, V_{j+1}, \ldots, V_{j+d}) = 1$ and $V_{j+n} = MV_j$, $j \in \mathbb{Z}$, where $M \in SL_{d+1}(\mathbb{C})$. (Strictly speaking, this lift is not unique, because it is defined up to a simultaneous multiplication of all vectors by $(-1)^{1/(d+1)}$, but the coordinates introduced below have the same values for all lifts.)[1]

---

[1] Note also that over $\mathbb{R}$ for odd d to obtain the lifts of n-gons from $\mathbb{RP}^d$ to $\mathbb{R}^{d+1}$ one might need to switch the sign of the monodromy matrix: $M \to -M \in SL_{d+1}(\mathbb{R})$, since the field is not algebraically closed. These monodromies correspond to the same projective monodromy in $PSL_{d+1}(\mathbb{R})$.

The coefficients of the following difference equation

$$V_{j+d+1} = a_{j,d}V_{j+d} + a_{j,d-1}V_{j+d-1} + \cdots + a_{j,1}V_{j+1} + (-1)^d V_j, \quad j \in \mathbb{Z}$$

turn out to be n-periodic in j due to the monodromy relation on vectors V_j, and, in particular, coefficients $\{a_{j,k} \mid j = 0, \ldots, n - 1, k = 1, \ldots, d\}$ play the role of the coordinates on the space $\mathcal{P}_n$. The dimension of the space $\mathcal{P}_n$ of generic n-gons in $\mathbb{CP}^d$ is dim $\mathcal{P}_n = nd$.

Now we are in a position to define Lax representations for the maps T_{sh} and T_m. The above pentagram maps can be presented in the Lax form $L_{j,t+1}(\lambda) = P_{j+1,t}(\lambda)L_{j,t}(\lambda)P_{j,t}^{-1}(\lambda)$ for an appropriate matrix $P_{j,t}(\lambda)$, where λ is a spectral parameter. We present the L matrices below, while the explicit expression for $P_{j,t}(\lambda)$ is complicated and is not required for our analysis.[2] The pentagram map corresponds to the time evolution $t \to t + 1$ of the Lax matrix.

Theorem 2.1 (=Theorem 1.4′). *Lax representations with a spectral parameter for the above pentagram maps are given by the following L-matrices:*

$$L_{j,t}(\lambda) = \begin{pmatrix} 0 & 0 & \cdots & 0 & (-1)^d \\ & & & & a_{j,1} \\ & & D(\lambda) & & a_{j,2} \\ & & & & \cdots \\ & & & & a_{j,d} \end{pmatrix}^{-1},$$

where $D(\lambda)$ is the following diagonal $(d \times d)$-matrix:

- *for the map T_{sh}, $D(\lambda) = \mathrm{diag}(\lambda, 1, \lambda, 1, \ldots, 1, \lambda)$ for odd d and $D(\lambda) = \mathrm{diag}(1, \lambda, 1, \ldots, 1, \lambda)$ for even d;*
- *for the map T_m, $D(\lambda) = \mathrm{diag}(1, \ldots, 1, \lambda, 1, \ldots, 1)$, where the spectral parameter λ is situated at the $(m + 1)$th place.*

The construction of a Lax representation for the deep-dented pentagram map $T_{m,p}$ relies on the lifting of generic polygons from $\mathbb{CP}^d$ to so-called partially corrugated polygons in a bigger space $\mathbb{CP}^{d+p-2}$. Then the corresponding Lax representation for the deep-dented maps can be obtained from the above Lax form for the map on generic polygons in $\mathbb{CP}^{d+p-2}$ by restricting it to the subset of partially corrugated ones, see details in [7].

3. Discrete integrability

The above Lax representation allows one to give a more detailed description of the dynamics. In particular, in low dimensions one can explicitly express the pentagram maps as a discrete dynamics on the Jacobian of the corresponding spectral curve. The following result is a corollary of that description.

Theorem 3.1. *The above integrable pentagram maps on twisted n-gons in $\mathbb{CP}^d$ cannot be included into a Hamiltonian flow as its time-one map, at least for some values of n, m, and d.*

Proof. In [3,5,7] we gave a detailed description of the pentagram maps T_{sh} and T_m in 2D and 3D (denote these maps by T_*). It turned out that for even n one observes the staircase-like dynamics on the Jacobian of the corresponding spectral curve. In the space $\mathcal{P}_n$ of generic twisted n-gons this corresponds to the following phenomenon. This space is a.e. fibered into (Zariski open subsets of) complex tori, which are invariant for the square T_*^2 of the pentagram map, but not for the map T_* itself. (More generally, the tori are invariant for a certain power T_*^q, while we set $q = 2$ for the rest of the proof.) In turn, the map T_* sends almost every n-gon from the space $\mathcal{P}_n$ to jump between two tori. The square of this map is a shift on each torus.

Now assume that such a map T_* were the time-one map of a smooth autonomous Hamiltonian field v on $\mathcal{P}_n$. Then this Hamiltonian field admits the same fibration a.e. into invariant tori, since T_*^2 is its time-two map and its frequencies are known to be nondegenerate. Then the flow of this field v would describe the linear evolution on tori, and hence it would be integrable itself. The map T_* is by assumption the time-one map of the same flow, and hence it must have the same invariant tori, rather than jumping between them. This contradiction proves that inclusion into a flow is impossible. □

Note that the dynamics of (partially) corrugated polygons, described in [7], allows jumps between 3 different tori for some values of n, m, p, and d.

We conjecture that the pentagram dynamics cannot be included into a flow for *all values* of n, m, and d (even when the above simple argument does not already work). The consideration and examples above suggest the following generalization of a discrete integrable Hamiltonian system. It can be regarded as a particular case of an integrable correspondence [8].

Definition 3.2. Suppose that (M, ω) is a $2n$-dimensional symplectic manifold and $I_1, \ldots, I_n$ are n independent functions in involution. Let $M_{\mathbf{c}}$ be a (possibly disconnected) level set of these functions: $M_{\mathbf{c}} = \{x \in M \mid I_j(x) = c_j, \ 1 \leq j \leq n\}$. A map $T : M \to M$ is called *generalized integrable* if

---

[2] One can recover the P-matrix from the coordinate formulas of the map and the fact that the ordered product $L_{n-1} \ldots L_1 L_0$ of L-matrices transforms by conjugation after the application of the map, see [5] for more details.

- it is symplectic, i.e., $T^*\omega = \omega$;
- it preserves the integrals of motion: $T^*I_j \equiv I_j$, $1 \le j \le n$;
- there exists a positive integer $q \ge 1$ such that the map T^q leaves all connected components of level sets $M_{\mathbf{c}}$ invariant for all $\mathbf{c} = (c_1, \ldots, c_n)$.

In other words, the qth iteration T^q of the map T is integrable in the usual sense. This definition lists almost verbatim the assertions of the Arnold–Liouville theorem [9] for continuous flows, which implies that one has a conditionally periodic motion for the map T^q and its "integrability by quadratures". The difference with the classical case, corresponding to $q = 1$, may occur if level sets $M_{\mathbf{c}}$ are disconnected, since the discrete map can "jump" from one component to another.

Our analysis (in the complexified case) shows that the pentagram maps T_{sh} for $d = 3$ and even n (in that case $q = 2$) and T_{cor} in the corrugated case for $d = 3$ and $n = 6l + 3$ (then one has $q = 3$) are generalized integrable. Note that compact connected components of generic level sets $M_{\mathbf{c}}$ are tori, and the map T can be used to establish an isomorphism of different connected components. Under such an isomorphism one obtains a "staircase" dynamics on the same torus (as discussed, e.g., in Theorem B in [3,5]).

4. Universal pentagram maps

In this section we define a general class of pentagram maps in any dimension, which allows one to intersect different diagonals at each step.

Definition 4.1. Let (v_k) be a generic twisted n-gon in $\mathbb{P}^d$. We fix d, pairwise different, d-tuples $I_1, \ldots, I_d$ of integers which are jump tuples defining d hyperplanes $P_k^{I_1}, \ldots, P_k^{I_d}$, i.e., each hyperplane $P_k^{I_\ell}$ passes through the vertices defined by its own jump d-tuple $I_\ell = (i_{\ell,1}, \ldots, i_{\ell,d})$:

$$P_k^{I_\ell} := (v_{k+i_{\ell,1}}, v_{k+i_{\ell,2}}, \ldots, v_{k+i_{\ell,d}}).$$

Now we define the *skew pentagram map* $T_{I_1,\ldots,I_d} : \mathscr{P}_n \to \mathscr{P}_n$, where vertices of a new n-gon are obtained by intersecting these d hyperplanes $P_k^{I_\ell}$, $\ell = 1, \ldots, d$:

$$T_{I_1,\ldots,I_d} v_k := P_k^{I_1} \cap P_k^{I_2} \cap \cdots \cap P_k^{I_d}.$$

Remark 4.2. (a) The general pentagram map $T_{I,J}$ described in Definition 1.5 is a particular case of the skew pentagram map $T_{I_1,\ldots,I_d}$: one can obtain both the jump $(d-1)$-tuple I and the intersection $(d-1)$-tuple J from the set of d-tuples $I_1, \ldots, I_d$.

(b) The pentagram maps in [10] are defined by intersecting a segment (v_{k-1}, v_{k+1}) with P_k^I for an appropriate choice of jumps I. This is a particular case of $T_{I_1,\ldots,I_d}$ with $I_d = I$, and d-tuples $I_1, \ldots, I_{d-1}$ all containing $(-1, +1, \ldots)$, so that all planes $P_k^{I_\ell}$ contain the pair of vertices (v_{k-1}, v_{k+1}), while their other vertices differ. In this case $P_k^{I_1} \cap P_k^{I_2} \cap \cdots \cap P_k^{I_{d-1}} = (v_{k-1}, v_{k+1})$.

In particular, the class of pentagram maps $T_{I_1,\ldots,I_d}$ with different d-tuples includes pentagram maps defined by taking intersections of subspaces of complimentary dimensions (and spanned by vertices (v_k)) to obtain a point as the intersection. For instance, the 3D map defined by the intersection $(v_k, v_{k+3}) \cap (v_{k+1}, v_{k+2}, v_{k+4})$ of a segment and a plane can be equivalently defined as the intersection of three planes: $(v_k, v_{k+3}, v_{k+5}) \cap (v_k, v_{k+3}, v_{k+6}) \cap (v_{k+1}, v_{k+2}, v_{k+4})$. Note that the intersections of hyperplanes provide a more general definition, since their intersection subspaces might not necessarily be spanned by vertices (v_k) themselves, but by their linear combinations.

Finally, define a universal pentagram map by starting with d polygons.

Definition 4.3. Let (v_k^ℓ) be d twisted polygons in $\mathbb{P}^d$, $\ell = 1, \ldots, d$ and $k \in \mathbb{Z}$, with the same monodromy matrix $M \in SL_{d+1}$. Now we fix two sets of d-tuples, jump tuples $I_1, \ldots, I_d$ and intersection tuples $J_1, \ldots, J_d$. Let $I_\ell = (i_{\ell,1}, \ldots, i_{\ell,d})$ and $J_p = (j_{p,1}, \ldots, j_{p,d})$. Define the hyperplane

$$P_k^{I_\ell} := (v_{k+i_{\ell,1}}^1, v_{k+i_{\ell,2}}^2, \ldots, v_{k+i_{\ell,d}}^d)$$

i.e., this plane $P_k^{I_\ell}$ uses one vertex from each n-gon. Now one can define d skew pentagram maps, or rather a *universal pentagram map*, whose image consists of d twisted n-gons: for every $p = 1, \ldots, d$ the map T_p uses the corresponding intersection tuple J_p:

$$T_p v_k := P_{k+j_{p,1}}^{I_1} \cap P_{k+j_{p,2}}^{I_2} \cap \cdots \cap P_{k+j_{p,d}}^{I_d}.$$

Thus one obtains a universal map $T_{\mathcal{I},\mathcal{J}}$ on d-tuples of twisted n-gons which is associated with two sets of tuples $\mathcal{I} = (I_1, \ldots, I_d)^t$ and $\mathcal{J} = (J_1, \ldots, J_d)^t$, where these sets $\mathcal{I} = (i_{\ell,s})$ and $\mathcal{J} = (j_{p,s})$ can be thought of as two $(d \times d)$-matrices composed of d-tuples $I_1, \ldots, I_d$ and, respectively, $J_1, \ldots, J_d$ written as their rows.

Theorem 4.4. *The universal pentagram maps possess the following duality:*

$$T_{\mathcal{I},\mathcal{J}}^{-1} = T_{-\mathcal{I}^*,-\mathcal{J}^*},$$

where $\mathcal{I}^*$ and $\mathcal{J}^*$ stand for the transposed matrices $\mathcal{I}^* = (i_{s,\ell})$ and $\mathcal{J}^* = (j_{s,p})$, respectively.

This duality generalizes the one (1.2) for the $T_{I,J}$ pentagram maps. Note that this theorem fully specifies the indices as opposed to the description in terms of jump $(d-1)$-tuples, which does not contain minuses, but gives a similar equality only up to a shift of indices.

Proof. To prove this theorem we modify the notion of a duality map, cf. [2,7].

Definition 4.5. Given d generic sequences of points $\phi_\ell(j) \in \mathbb{RP}^d$, $j \in \mathbb{Z}$, $\ell = 1, \ldots, d$ and a d-tuple $I = (i_1, \ldots, i_d)$ we define the following *sequence of hyperplanes* in $\mathbb{RP}^d$ enumerated by j:

$$\alpha_I(\phi_\star(j)) := (\phi_1(j + i_1), \phi_2(j + i_2), \ldots, \phi_d(j + i_d)),$$

which is regarded as a sequence of points in the dual space: $\alpha_I(\phi_\star(j)) \in (\mathbb{RP}^d)^*$, $j \in \mathbb{Z}$. For d tuples $I_1, \ldots, I_d$ we get d sequences $\alpha_{\mathcal{I}}(\phi_\star(j)) = (\alpha_{I_1}(\phi_\star(j)), \ldots, \alpha_{I_d}(\phi_\star(j))) \in (\mathbb{RP}^d)^* \times \cdots \times (\mathbb{RP}^d)^*$ enumerated by j. In other words, starting with d sequences of points in $\mathbb{RP}^d$, the map $\alpha_{\mathcal{I}}$ gives d sequences of points in the dual space $(\mathbb{RP}^d)^*$.

The universal pentagram map $T_{\mathcal{I},\mathcal{J}}$ on d twisted polygons can be defined as a composition of two such maps: $T_{\mathcal{I},\mathcal{J}} = \alpha_{\mathcal{I}} \circ \alpha_{\mathcal{J}}$. Note that these maps by definition possess the following duality property: $T_{\mathcal{I},-\mathcal{I}^*} = \alpha_{\mathcal{I}} \circ \alpha_{-\mathcal{I}^*} = \mathrm{Id}$.

For instance, in $\mathbb{RP}^2$ consider two twisted polygons (v_k^1) and (v_k^2) and two 2-tuples $I = (1, -2)$ and $I_2 = (-5, 3)$. Then in the dual space, by applying $\alpha_{\mathcal{I}}$ we obtain two twisted polygons, formed by lines $P_k^1 := (v_{k+1}^1, v_{k-2}^2)$ and $P_k^2 := (v_{k-5}^1, v_{k+3}^2)$. Then the vertex v_k^1 can be recovered from $v_k^1 = P_{k-1}^1 \cap P_{k+5}^2$, while $v_k^2 = P_{k+2}^1 \cap P_{k-3}^2$, i.e. by applying the map $\alpha_{-\mathcal{I}^*}$ to the sequences (P_k^1) and (P_k^2). Similarly this works in any dimension.

Now we see that

$$T_{\mathcal{I},\mathcal{J}} \circ T_{-\mathcal{J}^*,-\mathcal{I}^*} = \alpha_{\mathcal{I}} \circ \alpha_{\mathcal{J}} \circ \alpha_{-\mathcal{J}^*} \circ \alpha_{-\mathcal{I}^*} = \mathrm{Id},$$

as required. □

Note that if $\mathcal{J} = -\mathcal{J}^*$, i.e. the matrix $\mathcal{J}$ is skew-symmetric, then the map $\alpha_{\mathcal{J}}$ is an involution: $\alpha_{\mathcal{J}} \circ \alpha_{\mathcal{J}} = \mathrm{Id}$.

Corollary 4.6. *If $\mathcal{J}$ is skew-symmetric, then the pentagram maps $T_{\mathcal{I},\mathcal{J}}$ and $T_{\mathcal{J},\mathcal{I}}$ are conjugated to each other, i.e., the map $\alpha_{\mathcal{J}}$ takes the map $T_{\mathcal{I},\mathcal{J}}$ on d-tuples of twisted n-gons in $\mathbb{RP}^d$ into the map $T_{\mathcal{J},\mathcal{I}}$ on d-tuples of twisted n-gons in $(\mathbb{RP}^d)^*$. In particular, all four maps $T_{\mathcal{I},\mathcal{J}}$, $T_{-\mathcal{I}^*,\mathcal{J}}$, $T_{\mathcal{J},\mathcal{I}}$ and $T_{\mathcal{J},-\mathcal{I}^*}$ are integrable or non-integrable simultaneously.*

Proof. First note that

$$\alpha_{\mathcal{J}} \circ T_{\mathcal{I},\mathcal{J}} \circ \alpha_{\mathcal{J}}^{-1} = \alpha_{\mathcal{J}} \circ (\alpha_{\mathcal{I}} \circ \alpha_{\mathcal{J}}) \circ \alpha_{\mathcal{J}} = \alpha_{\mathcal{J}} \circ \alpha_{\mathcal{I}} = T_{\mathcal{J},\mathcal{I}}.$$

Hence the pentagram map $T_{\mathcal{I},\mathcal{J}}$ is conjugated to $T_{\mathcal{J},\mathcal{I}}$. Furthermore, the pentagram maps $T_{\mathcal{I},\mathcal{J}}$ and $T_{\mathcal{J},-\mathcal{I}^*}$, as well as $T_{\mathcal{J},\mathcal{I}}$ and $T_{-\mathcal{I}^*,\mathcal{J}}$, are inverses to each other for $\mathcal{J} = -\mathcal{J}^*$, as follows from Theorem 4.4. This proves the corollary. □

Conjecture 4.7. (a) *All universal pentagram maps $T_{\mathcal{I},\mathcal{J}}$ are discrete Hamiltonian systems (i.e., preserve a certain Poisson structure), although not necessarily integrable.*

(b) *A necessary condition for integrability of the universal pentagram maps $T_{\mathcal{I},\mathcal{J}}$ is their equivalence to a map $T_{I,J}$, see Definition 1.5.*

In the next two sections we provide a numerical evidence to Conjecture 4.7(b) and explain why this equivalence to an appropriate map $T_{I,J}$ cannot be sufficient for integrability.

5. Non-integrability in 2D

The classical case. In this section we are going to compare several pentagram maps in 2D. To detect integrability we use the height criterion following [11] (see more references on 'height' in [12]). Recall that the *height* of a rational number $a/b \in \mathbb{Q}$, written in the lowest terms, is $ht(a/b) = \max(|a|, |b|)$. We employ the cross-ratio coordinates (x, y) (defined in [2]) on the space of twisted n-gons $\mathcal{P}_n$ sitting inside $\mathbb{QP}^2$ (i.e., having only rational values of coordinates).

Definition 5.1. The *height* of a twisted n-gon $P \in \mathcal{P}_n$ in $\mathbb{QP}^2$ is defined as

$$H(P) := \max_{0 \le i \le n-1} \max(ht(x_i), ht(y_i)).$$

We trace how fast the height of an initial n-gon grows with the number of iterates of the pentagram map (i.e., with an integer parameter t). We perform the comparison for n-gons with $n = 11$. To specify a twisted 11-gon, we need 11 vectors in $\mathbb{Q}^3$ (which we then project to 11 vertices in $\mathbb{QP}^2$) and a monodromy from SL_3, which can be defined by fixing 3 more vectors in $\mathbb{Q}^3$. Overall we choose 14 vectors in $\mathbb{Q}^3$ uniformly distributed in $[1, 10]^3$.
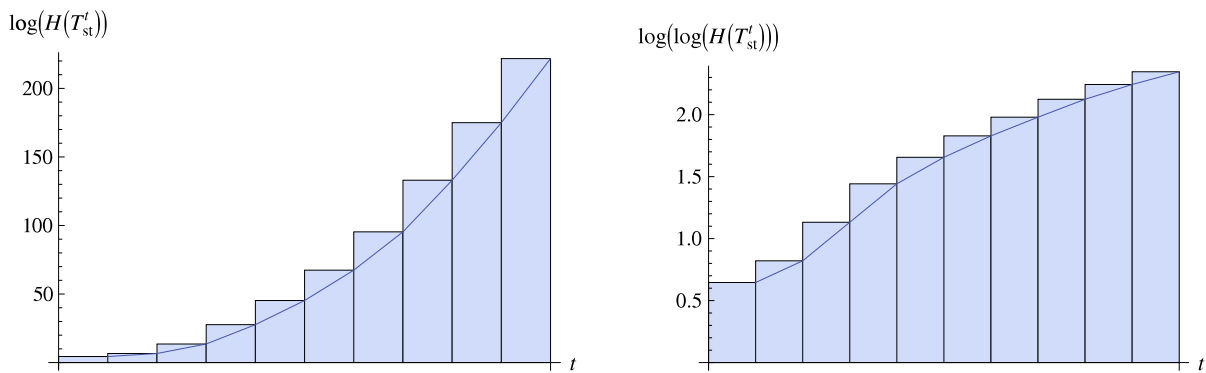
Fig. 3. Polynomial growth of $\log H$ for the map T_{st} in 2D as a function of t.

First, we start with the standard 2D pentagram map T_{st}. After 10 iterations, the height becomes of the order of 10^{250}. Because of its magnitude, it is natural to use the log scale and even the log–log scale for the height, see Fig. 3.

More generally, we are going to study the following $T_{I,J}$ maps in 2D with $I = (i)$ and $J = (j)$, where the diagonals are chords $P_k = (v_k, v_{k+i})$ and the maps are defined by intersecting those chords: $T_{I,J} v_k := P_k \cap P_{k+j}$.

Note that all these maps are integrable: the integrability of $T_{\mathrm{st}} := T_{(2),(1)}$ and of $T_{(3),(1)}$ follows from [2,4] (see also Theorem 1.4 in Section 1). The integrability in the case of $T_{(3),(2)}$, as well as of its dual $T_{(2),(3)} = T_{(3),(2)}^{-1} \circ Sh$, on 2D n-gons can be proved in a similar way by changing numeration of vertices, at least for n mutually prime with i or j and closed polygons. The integrability of such pentagram maps was also observed experimentally in the applet of R. Schwartz (personal communication).

In the table below we collected the order of magnitude for the height growth after 10 iterations for the following maps, see Fig. 4:

#	Notation for pent. map $T = T_{I,J}$	Definition of $T v_k$	Height H after 10 iterations
1.	$T_{\mathrm{st}} = T_{(2),(1)}$	$(v_k, v_{k+2}) \cap (v_{k+1}, v_{k+3})$	10^{320}
2.	$T_{(3),(1)}$	$(v_k, v_{k+3}) \cap (v_{k+1}, v_{k+4})$	10^{350}
3.	$T_{(3),(2)}$	$(v_k, v_{k+3}) \cap (v_{k+2}, v_{k+5})$	10^{750}
4.	$T_{(2),(3)}$	$(v_k, v_{k+2}) \cap (v_{k+3}, v_{k+5})$	10^{800}

The skew case. In all the cases above the pentagram maps were defined by taking intersections of the same type diagonals at each step. Now we generalize the definition of the classical 2D pentagram map to allow intersection of *different type* diagonals at each step.

As an example, we define the *skew pentagram map* on twisted polygons in $\mathbb{P}^2$ by intersecting at each step a short diagonal (v_k, v_{k+2}) of "length" 2 and a longer diagonal (v_{k+1}, v_{k+4}) of "length" 3: $\bar{T} v_k := (v_k, v_{k+2}) \cap (v_{k+1}, v_{k+4})$, see Fig. 5. (This map can be described as a universal map $T_{I,J}$ of Section 4, also cf. [10], where for any d one intersects a short diagonal with a hyperplane.) Note that the skew map $\bar{T}$ is not a generalized map of type $T_{I,J}$ from Definition 1.5 for any tuples I and J, as the latter maps were using the same definition of diagonals at each step. Now we are going to compare the height growth for this map $\bar{T}$, as well as for several similar maps, with that for the previously discussed integrable pentagram maps in 2D.

It turns out that for the skew map $\bar{T}$ after 10th iteration the height reaches the order of 10^{10^6}, see Fig. 6. The same order of magnitude for the height growth is observed for several similar maps, as summarized in the following table. We sketch the corresponding diagonals for these maps in Fig. 7.

#	Definition of $T v_k$	Height H after 10 iterations
5.	$\bar{T} v_k := (v_k, v_{k+2}) \cap (v_{k+1}, v_{k+4})$	10^{10^6}
6.	$(v_k, v_{k+2}) \cap (v_{k+1}, v_{k+5})$	10^{10^6}
7.	$(v_{k+1}, v_{k+2}) \cap (v_k, v_{k+3})$	10^{10^6}
8.	$(v_{k+1}, v_{k+2}) \cap (v_k, v_{k+4})$	10^{10^6}

Such a super fast growth is in sharp contrast with the classical integrable cases discussed earlier and suggests nonintegrability of all these skew pentagram maps.

Remark 5.2. Note that the above classical and skew examples are conjectured to be Hamiltonian, regardless of whether they are integrable or not, see Conjecture 4.7(a) and [7]. An example of a different type, the projective heat map in 2D, was proposed in [13]: it can be thought of as a dissipative system on polygons, while its continuous analog is the curvature flow
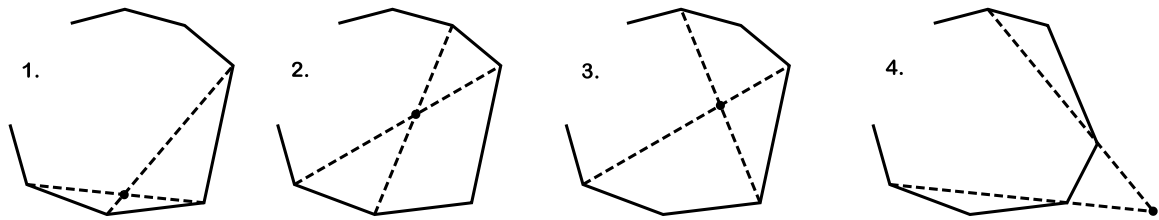
Fig. 4. The pentagram maps $T_{(i),(j)}$ on twisted polygons in 2D, where $T_{(i),(j)}v_k := (v_k, v_{k+i}) \cap (v_{k+j}, v_{k+i+j})$, cf. the table below: 1. $T_{(2),(1)}$, 2. $T_{(3),(1)}$, 3. $T_{(3),(2)}$, 4. $T_{(2),(3)}$.
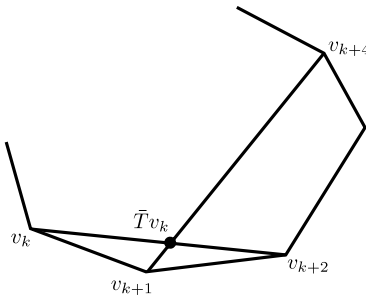

Fig. 5. The skew pentagram map $\bar{T}$ is obtained by intersecting diagonals of lengths 2 and 3 at each step.
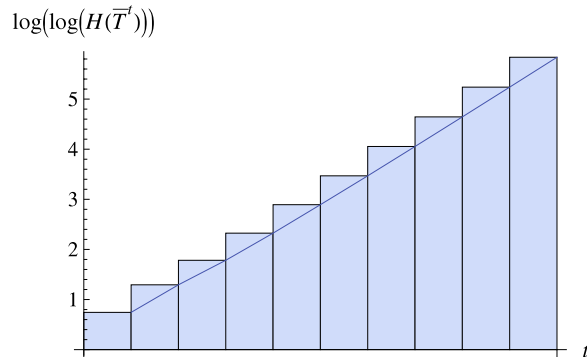

Fig. 6. Linear growth of log log H for the skew pentagram map $\bar{T}$ in 2D, which indicates super fast growth of its height.
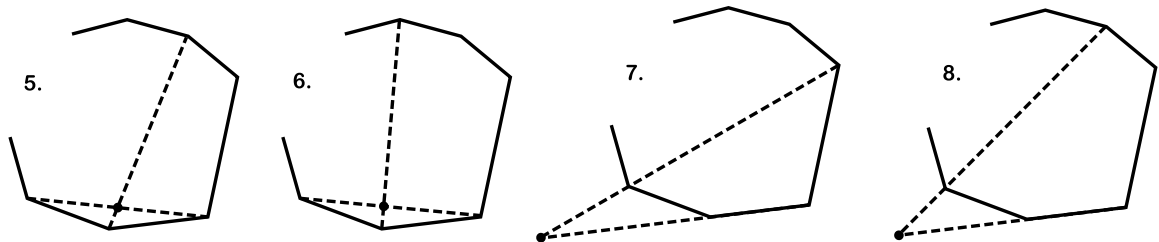

Fig. 7. The 2D pentagram maps with the following diagonals intersecting: 5. $(v_k, v_{k+2}) \cap (v_{k+1}, v_{k+4})$, 6. $(v_k, v_{k+2}) \cap (v_{k+1}, v_{k+5})$, 7. $(v_{k+1}, v_{k+2}) \cap (v_k, v_{k+3})$, 8. $(v_{k+1}, v_{k+2}) \cap (v_k, v_{k+4})$, cf. the table above.

on curves. This map turns out to converge to a (projectively) regular n-gon, at least for $n = 5$. Such a dynamical system cannot be integrable due to "dissipation", and this non-integrability is of a "non-Hamiltonian" nature.

6. Non-integrability in 3D

In this section we present the results of the numerical integrability test for various 3D pentagram maps. First of all, note that the definition of the height can be naturally extended to twisted rational polygons in any dimension. For instance, in
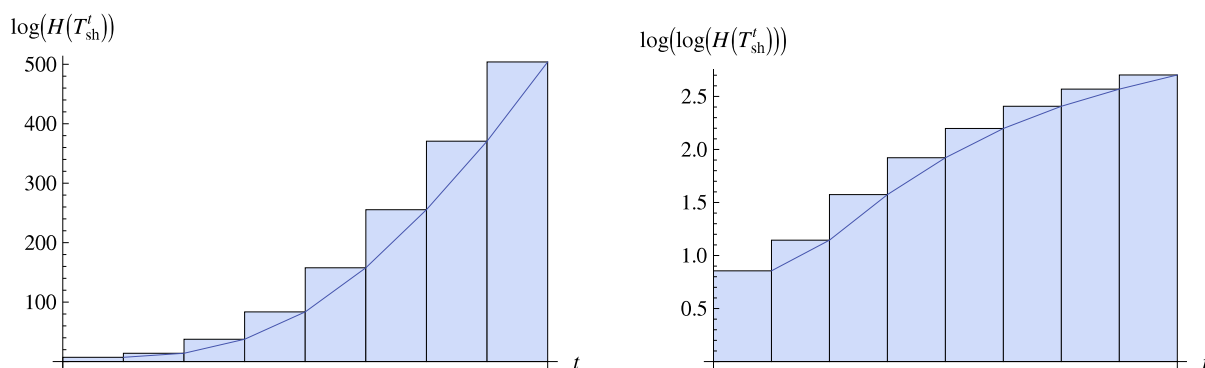
Fig. 8. Polynomial growth of $\log H$ for the integrable pentagram map T_{sh} in 3D as a function of t.

3D we employ the cross-ratio coordinates (x, y, z) (defined in [5]) on the space of twisted n-gons $\mathscr{P}_n$ in $\mathbb{P}^3$, with rational coordinates.[3]

Definition 6.1. The *height* of a twisted n-gon $P \in \mathscr{P}_n$ in $\mathbb{Q}\mathbb{P}^3$ is

$$H(P) := \max_{0 \leq i \leq n-1} \max(ht(x_i), ht(y_i), ht(z_i)).$$

Similarly to the above analysis we trace how fast the height of an initial n-gon for $n = 11$ grows with the number of iterates of different pentagram maps in 3D. Now we specify $15 = 11 + 4$ vectors in $\mathbb{Q}^4$ to fix a twisted 11-gon in $\mathbb{Q}\mathbb{P}^3$ and its monodromy from SL_4. Again, their coordinates are randomly distributed in $[1, 10]$.

It turns out that in 3D there also exists a sharp contrast in the height growth for different maps. However, the borderline between integrable and non-integrable ones does not lie between the classical and skew cases, and it is more difficult to describe. This is why we group the numerically integrable and non-integrable cases separately.

Numerically integrable 3D cases. We start this study with the short-diagonal map T_{sh} in 3D, which is known to be (algebraic–geometric) integrable [5]. After 8 iterations of this map, the height of the twisted 11-gon in $\mathbb{Q}\mathbb{P}^3$ becomes of the order of 10^{500}, see Fig. 8.

The height also grows moderately fast for another integrable map, dented map T_1, reaching the value of the order of 10^{800}. We also observe a similar moderate growth for the (integrable) deep-dented map $T_{m,p}$ in 3D with $m = 1$ and $p = 3$: the height remains around 10^{1000}.

The above cases correspond to taking intersections of consecutive planes, i.e., to $T_{I,J}$ with $J = (1, 1)$. One can also observe a moderate height growth for several pentagram maps with more elaborate tuples J. The results are collected in the following table:

#	Notation for pent. map $T = T_{I,J}$	Tv_k in 3D case	Height H after 8 iterations
1.	$T_{\mathrm{sh}} := T_{(2,2),(1,1)}$	$P_k = (v_k, v_{k+2}, v_{k+4})$, $Tv_k := P_k \cap P_{k+1} \cap P_{k+2}$	10^{500}
2.	$T_1 := T_{(2,1),(1,1)}$	$P_k = (v_k, v_{k+2}, v_{k+3})$, $Tv_k := P_k \cap P_{k+1} \cap P_{k+2}$	10^{800}
3.	$T_{1,3} := T_{(3,1),(1,1)}$	$P_k = (v_k, v_{k+3}, v_{k+4})$, $Tv_k := P_k \cap P_{k+1} \cap P_{k+2}$	10^{1000}
4.	$T_{(2,2),(1,2)}$	$P_k = (v_k, v_{k+2}, v_{k+4})$, $Tv_k := P_k \cap P_{k+1} \cap P_{k+3}$	10^{1000}
5.	$T_{(1,2),(1,2)}$	$P_k = (v_k, v_{k+1}, v_{k+3})$, $Tv_k := P_k \cap P_{k+1} \cap P_{k+3}$	10^{2000}
6.	$T_{(1,3),(1,3)}$	$P_k = (v_k, v_{k+1}, v_{k+4})$, $Tv_k := P_k \cap P_{k+1} \cap P_{k+4}$	10^{3000}
7.	$T_{(2,3),(2,3)}$	$P_k = (v_k, v_{k+2}, v_{k+5})$, $Tv_k := P_k \cap P_{k+2} \cap P_{k+5}$	10^{3000}

Remark 6.2. The first three cases in the table, with $J = (1, 1)$, have been proved to be integrable. The integrability of the other four, with non-unit J, is unknown. Also, the pattern, which differs these cases from the non-integrable ones discussed below is yet to be established.

---

[3] In any dimension one may use the quasi-periodic coordinates to construct cross-ratio-type coordinates, see [7].
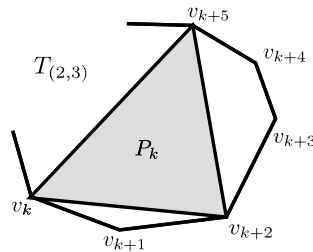
Fig. 9. The pentagram map $T_{(2,3)}$ in 3D is defined by intersecting three consecutive diagonals $P_k^{(2,3)} := (v_k, v_{k+2}, v_{k+5})$.
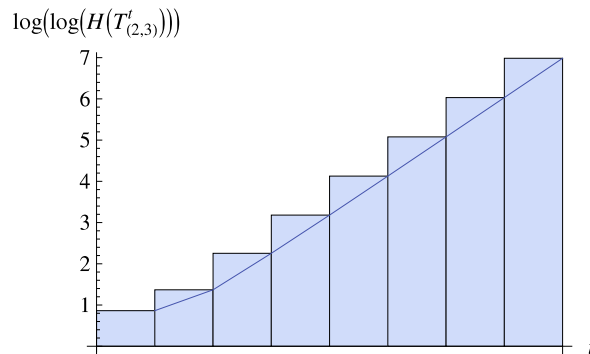

Fig. 10. Linear growth of log log H for the map $T_{(2,3)}$ in 3D indicating super fast growth of its height and apparent non-integrability.

Note that the case $T_{(2,2),(1,2)}$ has the "short" diagonal $P_k = (v_k, v_{k+2}, v_{k+4})$, and the pentagram map would be integrable for $J = (1, 1)$. However, here for $J = (1, 2)$ we take the intersection of two consecutive diagonals P_k's and one apart. (Similarly behaves the map $T_{(2,1),(2,2)}$, which is inverse of $T_{(2,2),(1,2)}$, and hence has the same integrability properties.) For the cases (5) and (6) in the table, their diagonals with $I = (1, 2)$ and $I = (1, 3)$ are also known to be integrable in combination with $J = (1, 1)$, while now the numerical results show that they are also integrable in combination with $J = (1, 2)$ and $J = (1, 3)$, respectively. Most surprisingly, the same holds for the case (7): the pentagram map for the diagonal $I = (2, 3)$ and the intersection $J = (2, 3)$ is now shown to be numerically integrable. The last three cases suggest the following conjecture.

Conjecture 6.3. *The pentagram maps $T_{I,I}$, i.e. those with $I = J$, are integrable.*

If proved, this would give a very large variety of integrable maps! (Note that T_{I,I^*} is always the identity map modulo a shift of indices, as follows from the properties of the duality maps, see [7]. In particular, e.g., one has $T_{(1,2),(2,1)} = Sh$.)

However, as we will see below, the same diagonals I in combination with other J's may give non-integrability: see the cases (8) and (9) in the table below, where one mixes $I = (1, 2)$ with $J = (3, 1)$ or $J = (1, 3)$. (Due to duality (1.2) one can interchange these I and J, which would lead to the same result on numerical non-integrability for $I = (1, 3)$ and $J = (2, 1)$.) Similarly, the diagonal $I = (2, 3)$ in combination with $J = (1, 1)$ is numerically non-integrable, see the case (10) below.

Numerically non-integrable 3D cases. Non-integrability of pentagram maps appears in several different situations. As we mentioned in Remark 6.2, it can be obtained by taking an "unusual" intersection tuple J with a "usually integrable" jump tuple I.

Another way to observe non-integrability is to choose a jump tuple I not covered by the integrability theorems (see the survey in Section 1). In 3D we proved integrability for pentagram maps defined by hyperplanes P_k of the following types: $P_k^{st} = (v_k, v_{k+2}, v_{k+4})$, $P_k^1 = (v_k, v_{k+2}, v_{k+3})$, $P_k^{1,p} = (v_k, v_{k+p}, v_{k+p+1})$ (and similarly for P_k^2 and $P_k^{2,p}$). One of the first cases not covered by these results is the pentagram map $T_{(2,3)} := T_{(2,3),(1,1)}$ in 3D defined by the hyperplanes $P_k^{(2,3)} := (v_k, v_{k+2}, v_{k+5})$ with the jump tuple $I = (2, 3)$, while $J = (1, 1)$, in notations of [7]:

$$T_{(2,3)}v_k := (v_k, v_{k+2}, v_{k+5}) \cap (v_{k+1}, v_{k+3}, v_{k+6}) \cap (v_{k+2}, v_{k+4}, v_{k+7}),$$

see Fig. 9. We conjectured in [7] (see also Conjecture 4.7(a)) that all maps defined by taking intersections of the same diagonals are discrete Hamiltonian. But they still might be non-integrable and $T_{(2,3)}$ is the first candidate for that. Here we present a numerical evidence for such a non-integrability.

The height growth turns out to be enormously faster for the map $T_{(2,3)}$ than for all integrable maps discussed above: after 8 iterations the height already reaches the order of magnitude of over 10^{10^7}, see Fig. 10. The map $T_{(2,3)}$ in 3D is a map defined by the same diagonal plane at each step, i.e., it is of type $T_{I,J}$. However, in a sense it is mimicking the skew map $\bar{T}$ in 2D defined by different type diagonals. More cases of presumably non-integrable maps are given in the table below. We

mention that the case (12) was discussed in [5], where the problem of its integrability was posed. It looked conjecturally integrable as the corresponding pentagram map $T_{(3,3),(1,1)}$ is the intersection of three consecutive very symmetric diagonals $P_k := (v_k, v_{k+3}, v_{k+6})$. However, the current numerical evidence suggests its non-integrability.

Finally, one more source of would-be non-integrable maps is skew pentagram maps, and, in particular, the maps constructed by intersecting different planes of complimentary dimensions at each step. The cases (13) and (14) in the table below illustrate the latter.

#	Tv_k in 3D case	Height H after 8 iterations
8.	$T_{(1,2),(3,1)}$	$10^{3 \cdot 10^7}$
9.	$T_{(1,2),(1,3)}$	$10^{3 \cdot 10^7}$
10.	$T_{(2,3)} := T_{(2,3),(1,1)}$	10^{10^7}
11.	$T_{(2,4)} := T_{(2,4),(1,1)}$	10^{10^7}
12.	$T_{(3,3)} := T_{(3,3),(1,1)}$	10^{10^7}
13.	$(v_k, v_{k+3}) \cap (v_{k+1}, v_{k+2}, v_{k+4})$	10^{10^6}
14.	$(v_{k+1}, v_{k+3}) \cap (v_k, v_{k+2}, v_{k+5})$	10^{10^6}

Remark 6.4. Note that all maps considered above can be expressed by rational functions. Apparently, in integrable cases many cancelations of different terms occur after several iterations, resulting in a much lower complexity, while one does not have those cancelations in non-integrable cases. It would be very interesting to prove the observed non-integrability directly, rather than numerically, possibly by employing Ziglin's or Morales–Ramis' methods.

The above consideration provides an evidence for Conjecture 4.7(b): a necessary condition for integrability of a pentagram map is to be of $T_{I,J}$-type, i.e., to be defined by intersections of the same-type diagonal hyperplanes at each step (see Definition 1.5). While the class of universal pentagram maps $T_{I,J}$ is very broad, all known *integrable* examples (such as short-diagonal, dented, deep-dented, corrugated and partially corrugated pentagram maps) can indeed be presented as $T_{I,J}$-type maps. However, this condition is not sufficient for integrability, as many examples of this section indicate.

Remark 6.5. It is often convenient to deal with the *logarithmic height* $h(T) := \log H(T)$ of a dynamical system T. The *arithmetic complexity* of a map T is defined as follows: $\delta(T) := \limsup_{n \to \infty} (h(T^n))^{1/n}$, see [14]. We observed that the quantity $\log \log H(T^n) = \log h(T^n)$ grows linearly with the number of iterations n for numerically non-integrable maps T, like $c \cdot n$ for $c > 0$, see Figs. 6 and 10. This allows one to predict that $h(T^n) \sim C^n$ with $C > 1$ as $n \to \infty$, and hence for such *non-integrable* maps there should be $\delta(T) = C > 1$.

On the other hand, sub-linear growth of $\log \log H(T^n) = \log h(T^n)$ for *integrable* maps T, see Figs. 3 and 8, indicates that apparently $\delta(T) = 1$ for them. We conjecture that the equality $\delta(T) = 1$ is a necessary condition for integrability of T in a more general setting:

Conjecture 6.6. *If a map T satisfies a Lax equation with a rational Lax matrix (i.e. rationally depending on coordinates and a spectral parameter), then the arithmetic complexity of this map satisfies $\delta(T) = 1$.*

Acknowledgments

References

[1] R. Schwartz, The pentagram map, Experiment. Math. 1 (1992) 71–81.
[2] V. Ovsienko, R. Schwartz, S. Tabachnikov, The pentagram map: a discrete integrable system, Comm. Math. Phys. 299 (2010) 409–446. arXiv:0810.5605.
[3] F. Soloviev, Integrability of the pentagram map, Duke Math. J. 162 (15) (2013) 2815–2853. arXiv:1106.3950.
[4] M. Gekhtman, M. Shapiro, S. Tabachnikov, A. Vainshtein, Higher pentagram maps, weighted directed networks, and cluster dynamics, Electron. Res. Announc. Math. Sci. 19 (2012) 1–17. arXiv:1110.0472.
[5] B. Khesin, F. Soloviev, Integrability of higher pentagram maps, Math. Ann. 357 (3) (2013) 1005–1047. arXiv:1204.0756.
[6] G. Marí-Beffa, On integrable generalizations of the pentagram map, IMRN (2014) 16. arXiv:1303.4295 http://dx.doi.org/10.1093/imrn/rnu044.
[7] B. Khesin, F. Soloviev, The geometry of dented pentagram maps, JEMS (2013) 32 in press arXiv:1308.5363.
[8] A. Veselov, Growth and integrability in the dynamics of mappings, Comm. Math. Phys. 145 (1) (1992) 181–193.
[9] V.I. Arnold, Mathematical Methods of Classical Mechanics, in: Graduate Texts in Mathematics, vol. 60, Springer, 1989.
[10] G. Marí-Beffa, On generalizations of the pentagram map: discretizations of AGD flows, J. Nonlinear Sci. 23 (2) (2013) 303–334. arXiv:1103.5047.
[11] R.G. Halburd, Diophantine integrability, J. Phys. A: Math. Gen. 38 (2005) L263–L269. arXiv:nlin/0504027.
[12] B. Grammaticos, R.G. Halburd, A. Ramani, C.-M. Viallet, How to detect the integrability of discrete systems, J. Phys. A: Math. Gen. 42 (2009) 454002. 30 pp.
[13] R. Schwartz, The projective heat map, Preprint, 2013, p. 32.
[14] S. Kawaguchi, J.H. Silverman, Examples of dynamical degree equals arithmetic degree, Michigan Math. J. 63 (1) (2014) 41–63. arXiv:1212.3015.